Published in final edited form as:
Mol Cell Neurosci. 2011 January ; 46(1): 159–166. doi:10.1016/j.mcn.2010.08.017.

Single-cell analysis of sodium channel expression in dorsal root ganglion neurons

Cojen Ho and **Michael E. O'Leary**
Department of Pathology, Anatomy and Cell Biology, Thomas Jefferson University, 1020 Locust Street, JAH 265, Philadelphia, PA 19107

Abstract

Sensory neurons of the dorsal root ganglia (DRG) express multiple voltage-gated sodium (Na) channels that substantially differ in gating kinetics and pharmacology. Small-diameter (<25 μm) neurons isolated from the rat DRG express a combination of fast tetrodotoxin-sensitive (TTX-S) and slow TTX-resistant (TTX-R) Na currents while large-diameter neurons (>30 μm) predominately express fast TTX-S Na current. Na channel expression was further investigated using single-cell RT-PCR to measure the transcripts present in individually harvested DRG neurons. Consistent with cellular electrophysiology, the small neurons expressed transcripts encoding for both TTX-S (Nav1.1, Nav1.2, Nav1.6, Nav1.7) and TTX-R (Nav1.8, Nav1.9) Na channels. Nav1.7, Nav1.8 and Nav1.9 were the predominant Na channels expressed in the small neurons. The large neurons highly expressed TTX-S isoforms (Nav1.1, Nav1.6, Nav1.7) while TTX-R channels were present at comparatively low levels. A unique subpopulation of the large neurons was identified that expressed TTX-R Na current and high levels of Nav1.8 transcript. DRG neurons also displayed substantial differences in the expression of neurofilaments (NF200, peripherin) and Necl-1, a neuronal adhesion molecule involved in myelination. The preferential expression of NF200 and Necl-1 suggests that large-diameter neurons give rise to thick myelinated axons. Small-diameter neurons expressed peripherin, but reduced levels of NF200 and Necl-1, a pattern more consistent with thin unmyelinated axons. Single-cell analysis of Na channel transcripts indicates that TTX-S and TTX-R Na channels are differentially expressed in large myelinated (Nav1.1, Nav1.6, Nav1.7) and small unmyelinated (Nav1.7, Nav1.8, Nav1.9) sensory neurons.

Keywords

Sodium channel; dorsal root ganglia; single-cell RT-PCR; Necl-1; NF200; peripherin

Introduction

The dorsal root ganglion (DRG) is composed of a heterogeneous population of neurons that convey a variety of sensory information from peripheral and visceral tissues to the central nervous system. DRG neurons have been classified according to the size of their cell bodies,

Corresponding Author: Dr. Michael E. O'Leary, Department of Pathology, Anatomy and Cell Biology, Thomas Jefferson University, 1020 Locust Street, JAH 265, Philadelphia, PA 19107, (215) 503-9983, Michael.oleary@jefferson.edu.

duration and amplitude of their action potentials, the extent of myelination, expression of neurofilaments and their axonal conduction velocities (Fornaro *et al.*, 2008;Goldstein *et al.*, 1991;Harper and Lawson, 1985;Lawson *et al.*, 1993;Lee *et al.*, 1986;Yoshida and Matsuda, 1979;Lawson, 2002). These studies indicate that the small-diameter DRG neurons (<30 μm) give rise to slowly-conducting unmyelinate(C) or thinly myelinated(Aδ) nerve fibers associated with thermoception and pain (Harper and Lawson, 1985). Large-diameter DRG neurons (>30 μm) have been linked to rapidly-conducting myelinated A fibers (Aα, Aβ), such as those typically associated with proprioception and low-threshold mechanoreception.

The small- and large-diameter neurons of the DRG express distinct populations of voltage-gated Na channels that govern the initiation and conduction of action potentials (Cummins *et al.*, 2007;Dib-Hajj *et al.*, 2009;Rush *et al.*, 2007). DRG Na currents have been broadly classified based on voltage-dependence, kinetics and pharmacology into rapidly-gating tetrodotoxin-sensitive (TTX-S), slowly-gating TTX-resistant (TTX-R) and persistent TTX-R components (Caffrey *et al.*, 1992;Elliott and Elliott, 1993;Kostyuk *et al.*, 1981;Roy and Narahashi, 1992). At least five distinct Na channel isoforms are known to be expressed in the DRG (Black *et al.*, 1996;Amaya *et al.*, 2000;Dib-Hajj *et al.*, 1998). Nav1.7 (PN1) encodes for a rapidly-gating TTX-S Na channel that is preferentially expressed in the dorsal root and sympathetic ganglia (Toledo-Aral *et al.*, 1997;Black *et al.*, 1996;Sangameswaran *et al.*, 1997). Nav1.7, along with several other isoforms (Nav1.1, Nav1.2, Nav1.6) account for the TTX-S Na current observed in most DRG neurons. Nav1.8 (PN3) encodes for a slowly-gating TTX-R Na current that is primarily expressed in small DRG neurons and produces the majority of the depolarizing inward current during action potentials (Akopian *et al.*, 1996;Blair and Bean, 2002;Sangameswaran *et al.*, 1996). The Nav1.9 channel (NaN) encodes for a slowly-gating Na channel that underlies a persistent TTX-R current in small DRG neurons (Dib-Hajj *et al.*, 1998;Tate *et al.*, 1998;Dib-Hajj *et al.*, 2002). The differential expression of these Na channels in small and large DRG neurons coupled with isoform-specific differences in voltage-dependence and gating kinetics are important determinants of neuronal excitability and the transmission of sensory information.

The goal of this study was to investigate Na channel expression in small- (<25 μm) and large-diameter (>30 μm) neurons acutely dissociated from the rat DRG. A combination of cellular electrophysiology and single-cell RT-PCR were used to compare the pharmacology and gating properties of the endogenous Na currents with the Na channel transcripts expressed in the same neurons. The neurons were further classified based on the expression of cytoplasmic neurofilaments (peripherin, NF200) and a cell adhesion molecule involved in myelination (Necl-1). The data indicate that small unmyelinated neurons express a combination of TTX-S (Nav1.7) and TTX-R (Nav1.8, Nav1.9) isoforms while large myelinated neurons preferentially express TTX-S (Nav1.1, Nav1.6, Nav1.7) channels.

Materials and Methods

DRG Cell Culture

Seven day old rat pups (male and female) were anaesthetized with isoflurane before decapitation and the dorsal root ganglia (DRG) harvested from all accessible levels. Ganglia were incubated for 30 min at 37°C in 2 ml of HBSS/HEPES containing 1.5 mg/ml collagenase (Sigma-Aldrich, St. Louis, MO) followed by 1 mg/ml trypsin (Sigma-Aldrich) for an additional 30 min. Trypsin was removed and the ganglia transferred to L-15 Leibovitz media supplemented with 1% fetal bovine serum (Gibco), 2 mM glutamine, 24 mM $NaHCO_3$, 38 mM glucose, 2% penicillin-streptomycin (Gibco), and 50 ng/ml nerve growth factor (Sigma-Aldrich). The ganglia were gently dissociated using fire-polished Pasteur pipettes and the neurons plated onto poly-L-lysine coated 35 mm dishes containing 2 ml of the supplemented L-15 media. Neurons were suitable for electrophysiology and harvesting

between 1 and 8 hours after plating. Animals were handled in accordance with the NIH guidelines and the protocols approved by the Animal Use and Care Committee of Thomas Jefferson University.

Electrophysiology

Whole-cell patch-clamp recordings of DRG neurons were made using sylgard-coated (Dow Corning Corp., Midland, MI) patch electrodes fashioned from Corning 8161 glass (Wilmad Glass Company, Buena, NJ). Series resistances ranged between 0.5 and 2 M2126 and were 80% compensated using the internal circuit of the Axopatch 200A. Currents are filtered at 10 kHz, digitized at 100 kHz and stored using pCLAMP software (Molecular Devices). Leak currents are subtracted using the P/4 procedure. Holding potentials were −80 mV unless otherwise stated. Pipette solution consisted of (in mM): 100 CsF, 25 CsCl, 10 NaCl, 1 EGTA, and 10 HEPES pH 7.4. Bath solution contained (in mM): 140 NaCl, 2 KCl, 1.5 $CaCl_2$, 1 $MgCl_2$, and 10 HEPES pH 7.4. Tetrodotoxin (TTX) was bath applied at a final concentration of 300 nM. For electrophysiology the neurons were initially sorted into small (≤25 μm) and large (≥30 μm) sizes using a micrometer scale superimposed on the visual field. A more accurate estimate of neuronal diameter was obtained from measurements of whole-cell capacitance assuming a specific membrane capacitance of 1 $\mu F/cm^2$ and spherical shape (Hamada et al., 2003).

Quantitative real-time PCR

Intact DRG neurons were harvested by drawing the cells into large bore pipettes (≈20 μm diameter) containing 10 μl of RNase-free water. The cell lysates were ejected into a sterile PCR tube and rapidly frozen. Random hexamer primers (65 ng, Invitrogen) were added and the sample heated to 70°C for 3 minutes before transfer to ice. mRNA was reverse transcribed (RT) in a 25 μl reaction containing MMLV reverse transcriptase (200 units, Fischer Bioreagents), 50 mM Tris-HCl (pH 8.3), 75 mM KCl, 3 mM $MgCl_2$, 10 mM dithiothreitol, 0.5 mM dNTPs and RNase Inhibitor (1 unit/μl, Promega). Na channel cDNA (Nav1.1– Nav1.9) present in aliquots of the RT reactions (1–3 μl) were measured with TaqMan probes (Applied Biosystems) on a Mx3005P real-time PCR machine (Agilent Technologies). Depending on Na channel expression level the cell lysates yielded cutoff cycles (Ct) ranging between 32 and 38 cycles. Real-time amplification was not observed (No Ct value) when reverse transcriptase was omitted from the reaction (RT-) or when samples of the bath solution immediately surrounding the harvested neurons was assayed. The absolute number of mRNA copies was determined by comparing the Ct values of the cell lysates to those of known cDNA standards generated from PCR fragments of Na channel cDNA. Standard cDNA was obtained from RT-PCR of mRNA extracted from intact DRG. Standard primer sets were designed to generate cDNA fragments (≈400 bp) spanning the Taqman detection sites. Standard cDNA was amplified in 25 μl PCR reactions using 1 μl of RT reaction, 200 nM gene-specific Na channel primers, 1 unit Taq polymerase (Roche), 10 mM Tris-HCl (ph 8.3), 1.5 mM $MgCl_2$ and 50 mM KCl. The resulting PCR standard fragments were isolated on 2% agarose gels and purified using Qiaex II columns (Qiagen). The number of cDNA copies (copies/μl) was calculated from the OD_{260}, PCR fragment length and average molecular weight of a double-stranded DNA molecule (660 gms/mole). Plots of the standard cDNA copy number versus Ct value were semi-logarithmic between 10 and 10^6 cDNA copies and routinely had efficiencies between 90 and 105%. The number of Na channel mRNA copies present in the cell lysates was corrected for variation in sample handling by normalizing the β actin Ct values of the individual samples to the mean β actin Ct value of the sample population. The number of Na channel mRNA copies per neuron is expressed as the mean and standard error of the mean (SEM).

The forward (f) and reverse (r) primers used for generating cDNA standards were:

Nav1.1 (f) CGCTGTCATCCTGGAGAACT, (r) TCCTTCCTGCTCGTGTTTCT;

Nav1.2 (f) GGGAGAAGTTCGACCCTGAC, (AS) TTCCCTGATATCTTTCCCTTTG;

Nav1.5 (f) AGATGACCAGAGCCCTGAGA, (r) GCGAAGGTCTGGAAGTTGAA;

Nav1.6 (f) CATGTACATCGCCATCATCC, (r) GCTGCTGCTTCTCCTTGTCT;

Nav1.7 (f) CGCTGTCATCCTGGAGAACT, (r) GTCATAGGAAGGTGGCGAGA;

Nav1.8 (f) TGAGACCTGGGAGAAGTTCG, (r) AGCAGCGACCTCATCTTCAT;

Nav1.9 (f) TCTCCTTCCTCATCGTGGTC, (r) AAGCTGTGAGGCAGTGAGGT;

β actin (f) GCTATGTTGCCCTAGACTTCG, (r) AACGCAGCTCAGTAACAGTCC;

Peripherin (f) ATCTCAGTGCCCGTTCATTC, (r) AGCAGGACTGGTTGCAGACT;

NF200 (f) GCAGTCAGAGGAGTGGTTCC, (r) TCTCAATATCCAGGGCCATC;

Necl1 (f) AGACGCGAATCCAGGAAGAT, (r) GGCTGTATAGCTGCCCATGT.

Results

Cellular electrophysiology of DRG neurons

Figure 1A shows the whole-cell Na current of a small-diameter (25 μm) neuron acutely dissociated from the rat DRG. The currents began activating around −40 mV and inactivated with a time constant (τ_h) of 0.97 ± 0.03 ms at +20 mV (n=13). Tetrodotoxin (TTX) was a relatively weak inhibitor of this Na current reducing the peak amplitude by 19.7 ± 1.0 % (n=13) (Figure 1B). The whole-cell capacitances of these small neurons ranged between 15 and 24 pF corresponding to a cell body diameter of 24.9 ± 0.5 μm (n=13). Figure 1C shows the Na current of a large-diameter (35 μm) neuron measured under identical conditions. These Na currents began activating at relatively hyperpolarized voltages (≈ −60 mV) and rapidly inactivated with a time constant (τ_h) of 0.40 ± 0.13 ms (n=8). TTX inhibited the majority of this Na current (99.4 ± 2.0 %, n=14) consistent with the preferential expression of TTX-sensitive (TTX-S) Na channels in this population (Figure 1D). The whole-cell capacitance of these neurons ranged between 30 and 69 pF corresponding to a diameter of 38.9 ± 1.2 μm (n = 12).

The normalized conductance was calculated from the peak Na currents of small and large neurons and plotted versus the test potential (Figure 2A). The smooth curves are fits of the data to a double Boltzmann function with midpoints (V_{act}) of −26 mV and −15 mV for the small neurons and −38 mV and −29 mV for the large neurons. Also plotted is the steady-state inactivation determined using 500 ms prepulses to voltages between −120 and −30 mV. The smooth curves are fits to a double Boltzmann with midpoints (V_{in}) of −66 mV and −40 mV for the small neurons and −103 mV and −68 mV for the large neurons. The activation and steady-state inactivation of both populations was a composite of two or more components suggesting that multiple Na channels contribute to the whole-cell currents in these neurons.

The Na currents of these neurons were further characterized by individually measuring the properties of the TTX-S and TTX-R components. The TTX-S currents of the large neurons were isolated by subtracting the residual TTX-R current measured after the bath application of TTX from the total Na current. The normalized conductance and steady-state inactivation of these currents were determined and plotted versus the test potential (Figure 2B). The smooth curves are fits to Boltzmann functions with midpoints of activation (V_{act}) and inactivation (V_{in}) of −23 mV and −67 mV respectively (Figure 2B). The voltage-dependent

gating of the isolated TTX-S current is similar to components of Na current measured in both the small (V_{act}= −26 mV, V_{in}= −66 mV) and large (V_{act}= −29, V_{in}= −8 mV) neurons (Figure 2A). This finding is consistent with work showing that TTX-S Na channels with similar gating properties are widely expressed in DRG neurons (Cummins et al., 2007;Rush et al., 2007).

The TTX-R current of small-diameter neurons was directly measured after bath application of TTX. The midpoint of activation (V_{act}) was −12 mV while the steady-state inactivation was best fitted with a double Boltzmann function with midpoints (V_{in}) of −76 mV and −30 mV (Figure 2B). The majority (90%) of the inactivation was associated with the more depolarized (V_{in}= −30 mV) component. The activation and inactivation of the isolated TTX-R current displayed properties similar to the predominant TTX-R current (V_{act}= −15 mV, V_{in}= −40 mV) preferentially expressed in small neurons (Figure 2A).

In addition to the slowly-inactivating TTX-R Na current, DRG neurons also express a persistent TTX-R component (Baker and Bostock, 1997;Cummins *et al.*, 1999). This current was isolated by pre-treating with A-803467, a selective Nav1.8 channel inhibitor (Jarvis et al., 2007), to reduce the more dominant slowly-inactivating TTX-R current (Figure 3A). Holding the neurons at relatively depolarized voltages (−60 mV) promotes the slow inactivation of the persistent Na current that only slowly recovers at hyperpolarized voltages (Cummins et al., 1999). Applying short hyperpolarizing prepulses (−140 mV/25 ms) prior to the test pulses permitted the full recovery of the inactivating but not the persistent component (Figure 3B). Figure 3C shows the persistent TTX-R Na current obtained by subtracting the inactivating component (Panel B) from the total current (Panel A). The resulting Na currents slowly inactivated at −20 mV with a time constant (τ_h) of 41 ± 6 ms, had a peak current density of 176 ± 29 pA/pF (n=8) and activated with a midpoint ($V_{0.5}$) of −39 mV (Figure 3D). These properties are similar to what has been previously reported for the persistent TTX-R Na currents of DRG neurons (Cummins *et al.*, 1999; Dib-Hajj *et al.*, 2002;Coste *et al.*, 2004;Priest *et al.*, 2005).

Single-cell analysis of the Na channel transcripts

To further characterize Na channel expression the mRNA present in individually harvested small and large DRG neurons was quantitatively measured using real-time PCR. The number of mRNA copies present in the cell lysates was obtained by comparing the cutoff cycle (Ct) values of the samples with those of known cDNA standards (Methods). Figure 4A compares the mRNA expression (copies/neuron) of small- (<25 μm) and large-diameter (>30 μm) neurons. Small neurons expressed mRNA encoding for both TTX-S (Nav1.7) and TTX-R (Nav1.8, Nav1.9) Na channels. Transcripts encoding for several other TTX-S isoforms (Nav1.1, Nav1.2, Nav1.6) were also detected in the small neurons but were present at comparatively low levels suggesting that Nav1.7 is the predominant TTX-S Na channel expressed in this population. The prevalent expression of Nav1.7, Nav1.8 and Nav1.9 channels is consistent with electrophysiology showing that small-diameter neurons express a combination of TTX-S and TTX-R Na currents (Figure 1). This contrasted with the large-diameter neurons that displayed prominent TTX-S Na current (Figure 1) and expressed mRNA encoding for the TTX-S (Nav1.1, Nav1.6, Nav1.7) isoforms (Table 1). Paradoxically, these large neurons also displayed high levels of Nav1.8 mRNA (Figure 4A) despite the absence of TTX-R Na current in the vast majority (80%) of these neurons. The expression of TTX-R Na channels in a subpopulation of the large neurons is examined in more detail in the next section.

A particular strength of the single-cell measurements is that it permits analysis of multiple Na channel transcripts from individual neurons thereby providing a quantitative assessment of isoform expression at the cellular level. Small and large neurons were individually

harvested and assayed for TTX-S (Nav1.1, Nav1.6, Nav1.7) and TTX-R (Nav1.5, Nav1.8, Nav1.9) Na channels. Small neurons highly expressed Nav1.7, but comparatively few copies of Nav1.1 or Nav1.6 mRNA (Figure 4B). This contrasted with the large neurons that broadly expressed mRNA for all three of the TTX-S isoforms. Figure 4C shows a similar analysis of the TTX-R Na channels. The small neurons highly expressed Nav1.8 and Nav1.9 while the large neurons expressed variable quantities of Nav1.8 and low levels of Nav1.9. Nav1.5 was detected in very few of the neurons (14%) and was present at comparatively low copy numbers (11 ± 5 copies/neuron, n=71).

Nav1.8 channels are highly expressed in a subpopulation of the large neurons

Whole-cell recordings indicated that the Na currents of small neurons were relatively insensitive to externally applied TTX while large neurons preferentially expressed TTX-S Na current (Figure 1). This conflicted with transcript analysis indicating that TTX-R Nav1.8 channel mRNA was present at comparably high levels in both populations (Figure 4A). However, single-cell analysis shows that Nav1.8 mRNA displays an unusually broad distribution in the large neurons (Figure 4C). The majority (78%) expressed Nav1.8 mRNA at moderate levels (1016 ± 120 copies/neuron) while the remaining fraction (22%) displayed considerably higher copy numbers (7439 ± 525 copies/neuron, n=20). A similar broad distribution of Nav1.8 mRNA in larger-diameter neurons has been observed using *in situ* hybridization (Fukuoka et al., 2008). Together these data suggest that Nav1.8 channels may be highly expressed in a subpopulation of the large neurons.

Figure 5 shows an example of a large-diameter (40 μm) neuron expressing TTX-R Na current. The cell bodies of neurons expressing this current had diameters typical of large neurons (38.8 ± 1.4 μm) but had Na currents that were weakly inhibited by TTX (24.3 ± 4.5%, n=14). To further investigate this unique population the TTX-R current of large neurons were normalized to the whole-cell capacitance (pA/pF) and plotted as a frequency histogram (Figure 5C). Consistent with two populations the TTX-R current histograms were bimodal with peaks at 17 and 232 pA/pF. This contrasted with the current density histograms of the small neurons that displayed a single peak around 379 pA/pF, consistent with a more uniform distribution of TTX-R channels in this population (Figure 5D).

The molecular basis of this 10-fold difference in TTX-R current density was further investigated using Na current measurements to determine the TTX sensitivity of large neurons before harvesting and mRNA analysis. The voltage-dependent activation ($V_{0.5}$ = −11.7 ± 1.2 mV, n=6) and inactivation time constants (τ_h = 1.2 ± 0.2 ms at +20 mV, n=6) of the TTX-R Na currents in these large neurons were similar to what was previously observed for the predominant TTX-R current of small neurons ($V_{0.5}$ = −11.7 ± 0.8 mV, τ_h = 1.0 ms) suggesting that Nav1.8 expression may underlie these currents. Figure 5E shows that the real-time PCR amplification of Nav1.8 mRNA from large neurons segregates into two populations consistent with low and high expression of Nav1.8 channels. Quantitative analysis showed that large neurons displaying TTX-R current (157 ± 44 pA/pF, n=5) expressed Nav1.8 mRNA at 5-fold higher levels than those with small TTX-R currents (22 ± 11 pA/pF, n=6). Although Nav1.9 mRNA was also elevated in this population, no persistent TTX-R current was observed and Nav1.9 expression levels (671 ± 160 copies/neuron, n=10) were nearly 5-fold lower than what is typically observed in small neurons (2854 ± 238 copies/neuron, n=71) where these currents are routinely observed.

Molecular markers of small unmyelinated and large myelinated neurons

Cytoplasmic neurofilaments contribute to the neuronal cytoskeleton, provide structural integrity and are important determinants of the axonal diameter and the velocity of impulse conduction along peripheral nerve fibers (Hoffman *et al.*, 1985;Fuchs and Cleveland, 1998).

The heavy neurofilament NF200 (200 kDa) and intermediate neurofilament peripherin (57 kDa) are preferentially expressed in large and small DRG neurons respectively and have proved to be useful markers for distinguishing between these populations (Goldstein *et al.*, 1991;Fornaro *et al.*, 2008). Consistent with these expectations peripherin mRNA was found to be present at 1.7-fold higher levels in small neurons while NF200 mRNA was 20-fold higher in the large neurons (Figure 6).

Necls are a family of cell adhesion molecules that mediate axonal-glial interactions (Spiegel *et al.*, 2007;Maurel *et al.*, 2007). Heterophilic interaction between Necl-1 of peripheral neurons and Necl-4 of Schwann cells promotes the formation of myelin sheaths. Figure 6 shows that Necl-1 mRNA is preferentially expressed in large neurons. The combination of NF200 and Necl-1 mRNA suggests that these large neurons may give rise to thick myelinated axons. Conversely, the small neurons express peripherin but comparatively little NF200 or Necl-1 suggesting that these neurons may be associated with thin unmyelinated axons.

Discussion

DRG sensory neurons express multiple Na channel isoforms that substantially differ in voltage-dependence, kinetics and pharmacology (Cummins *et al.*, 2007;Lai *et al.*, 2004;Rush *et al.*, 2007). These Na channels are differentially expressed in subpopulations of DRG neurons where they contribute to excitability and regulate action potential firing. Previous studies have employed a variety of techniques including electrophysiology, immunohistochemistry and *in situ* hybridization to investigate Na channels expression in these neurons (Caffrey *et al.*, 1992;Elliott and Elliott, 1993;Kostyuk *et al.*, 1981;Roy and Narahashi, 1992;Amaya *et al.*, 2000;Black *et al.*, 1996;Fjell *et al.*, 2000;Fukuoka *et al.*, 2008;Sangameswaran *et al.*, 1996;Toledo-Aral *et al.*, 1997). These studies have been instrumental in identifying the expressed Na channel isoforms and characterizing their contributions to sensory neuron excitability. The goal of this study was to build on this previous work by employing single-cell RT-PCR to compare Na channel mRNA expression in small and large DRG neurons. This approach is advantageous because it permits the measurement of multiple Na channel transcripts from each harvested neuron thereby enabling a highly quantitative analysis of Na channel expression in identified subpopulations of DRG neurons.

Expression of Na channel in small DRG neurons

The small-diameter (<25 μm) neurons isolated from the rat DRG express a combination of TTX-S and TTX-R Na current (Figure 1). The predominant TTX-R current present in these neurons activated and inactivated over a relatively depolarized range of voltages (Figure 2) and displayed slow gating kinetics (Figure 1). These Na currents were observed in virtually all small neurons and displayed properties similar to what has been previously reported for endogenous TTX-R Na currents (Caffrey *et al.*, 1992;Elliott and Elliott, 1993;Kostyuk *et al.*, 1981;Roy and Narahashi, 1992) and heterologously expressed Nav1.8 channels (Vijayaragavan *et al.*, 2001;Choi *et al.*, 2004;John *et al.*, 2004;Leffler *et al.*, 2007). A second smaller component of TTX-R current was observed to activate at relatively hyperpolarized potentials (−60 mV) and remained open during prolonged (>200 ms) depolarization (Figure 3C). The slow kinetics, incomplete inactivation and low activation threshold are consistent with previous studies of Nav1.9 channels (Cummins *et al.*, 1999;Dib-Hajj *et al.*, 2002;Coste *et al.*, 2004;Priest *et al.*, 2005). The TTX-S currents of small-diameter neurons accounted for a relatively minor fraction of the peak Na conductance (Figure 1). Unlike the TTX-R currents produced by the Nav1.8 and Nav1.9 channels, which display unique gating behaviors, the multiple overlapping components of TTX-S current of small neurons have

similar voltage-dependence and gating kinetics, significantly complicating attempts to identify the Na channel isoforms that produce these currents.

Na channel expression was further investigated using single-cell RT-PCR to quantitatively measure the mRNA present in small neurons (Figure 4A). Transcripts encoding for the Nav1.8 and Nav1.9 channels were highly expressed in the small neurons consistent with the presence of slowly inactivating and persistent components of TTX-R Na currents in this population. These data are in good agreement with previous work showing that both Nav1.8 and Nav1.9 are preferentially expressed in small-diameter DRG neurons (Sangameswaran *et al.*, 1996;Amaya *et al.*, 2000;Dib-Hajj *et al.*, 1998;Fang *et al.*, 2002;Fjell *et al.*, 2000;Tate *et al.*, 1998). Nav1.5 was detected in a small percentage of the neurons (11%) and at low copy numbers (<20 copies/neuron) indicating that these channels do not significantly contribute to the TTX-R Na current. The small neurons also expressed transcripts encoding for several TTX-S Na channels (Nav1.1, Nav1.2, Nav1.6, Nav1.7). However, Nav1.7 mRNA was present at 9–16 fold higher levels than the other isoforms suggesting that it is the predominant TTX-S Na channel expressed in the small neurons. These findings are consistent with previous work showing that Nav1.7 is widely expressed in DRG neurons (Black *et al.*, 1996;Fukuoka *et al.*, 2008) and in functionally identified nociceptors (Djouhri et al., 2003).

Na channel expression in large DRG neurons

The Na currents of large-diameter (≥30 μm) neurons displayed rapid kinetics and gated over a relatively hyperpolarized range of voltages (Figure 1). These currents were inhibited by nanomolar concentrations of TTX indicating the prevalence of TTX-S isoforms in these neurons. Single-cell analysis demonstrated that Nav1.1, Nav1.6 and Nav1.7 mRNAs were expressed at comparable levels in these neurons (Figure 4A). Previous work has shown that Nav1.1 and Nav1.6 channels are preferentially expressed in medium and large DRG neurons but in relatively few of the small neurons (Black *et al.*, 1996;Fukuoka *et al.*, 2008;Sangameswaran *et al.*, 1996). This contrasts with Nav1.7, which is broadly expressed in all DRG neurons (Black et al., 1996) and in approximately 70% of the large neurons (Fukuoka et al., 2008). These findings indicate that Nav1.1, Nav1.6 and Nav1.7 channels underlie the majority of the TTX-S Na current in large DRG neurons. This expression pattern may be significant since Nav1.6 and Nav1.7 channels heterologously expressed in sensory neurons display substantial differences in closed-state inactivation and recovery from inactivation (Herzog *et al.*, 2003). Differential expression of these isoforms may regulate the action potential threshold and firing frequency of large sensory neurons.

Electrophysiology identified a subpopulation of the large neurons that expressed TTX-R Na current with similar voltage dependence and kinetics as the TTX-R current of small neurons (Figure 5). Large neurons expressing this TTX-R current were individually harvested and analyzed for mRNA content. Neurons displaying TTX-R current expressed Nav1.8 and Nav1.9 transcripts at 4–5 fold higher levels than the general population of large neurons (Figure 5F). The voltage-dependent gating properties, TTX sensitivity and transcript analysis support the conclusion that Nav1.8 channels underlie the TTX-R Na current in this subpopulation. Despite increased expression of Nav1.9 mRNA, whole-cell recordings failed to detect persistent TTX-R Na current in these large neurons.

Previous studies found that 10–30% of large-diameter DRG neurons display Nav1.8 immunolabelling (Amaya *et al.*, 2000;Djouhri *et al.*, 2003), contain Nav1.8 transcript (Black *et al.*, 2004;Sangameswaran *et al.*, 1996;Novakovic *et al.*, 1998) or express TTX-R Na current with properties similar to those of Nav1.8 channels (Tate *et al.*, 1998;Sangameswaran *et al.*, 1996;Renganathan *et al.*, 2000). In addition, Nav1.8 expression overlaps with NF200, a neurofilament preferentially expressed in large-diameter neurons

(Lawson *et al.*, 1993;Novakovic *et al.*, 1998;Perry *et al.*, 1991;Fukuoka *et al.*, 2008). In this study, large neurons with prominent TTX-R Na currents also had high levels of NF200 and Necl-1 mRNA encoding for proteins typically associated with rapidly-conducting myelinated nerve fibers (Lawson *et al.*, 1993;Maurel *et al.*, 2007;Spiegel *et al.*, 2007). The data indicate that in addition to its broad distribution in small unmyelinated neurons, Nav1.8 is highly expressed in a subpopulation of large myelinated neurons (Renganathan *et al.*, 2000;Djouhri *et al.*, 2003).

Differential expression of neurofilaments and myelin-associated adhesion molecules

DRG neurons have been broadly classified based on the size of the cell bodies, axonal diameters and the velocity of action potential conduction (Yoshida and Matsuda, 1979;Harper and Lawson, 1985;Lawson *et al.*, 1993;Lee *et al.*, 1986). These neurons have been further differentiated based on the expression of NF-200 and peripherin, cytoplasmic neurofilaments that are preferentially expressed in large- and small-diameter nerve fibers respectively (Fornaro *et al.*, 2008;Goldstein *et al.*, 1991;Perry *et al.*, 1991). Neurofilament density is an important determinant of both axonal caliber and nerve fiber conduction velocity (Hoffman *et al.*, 1987;Lasek *et al.*, 1983;Lawson and Waddell, 1991). In this study the large neurons were found to express NF200 mRNA at 20-fold higher levels than small neurons supporting the idea these large neurons give rise to thick rapidly-conducing axons (Figure 6). This contrasted with the small neurons, which expressed peripherin at higher levels than the large neurons but displayed substantially reduced levels of NF200 (Figure 6), a profile that is more consistent with thin slowly-conducting axons.

Necl-1 is a neuronal adhesion molecule that forms heterophilic interactions with Necl-4 of Schwann cells and plays an important role in glial differentiation and myelination of peripheral nerve fibers (Maurel *et al.*, 2007;Spiegel *et al.*, 2007;Kakunaga *et al.*, 2005). Single-cell analysis indicates that Necl-1 mRNA is present at 10-fold higher levels in the large neurons suggesting that the axons arising from these cell bodies are likely to be myelinated (Figure 6).

Conclusions

This study employed electrophysiology and single-cell RT-PCR to investigate Na channel expression in identified populations of DRG sensory neurons. The ability to quantitatively analyze multiple transcripts from single neurons enabled a comparison of the pharmacology and gating properties of the endogenous Na currents with the Na channel isoforms expressed in the same neurons. Small-diameter (<25 μm) DRG neurons displaying prominent TTX-R Na currents co-expressed both TTX-S and TTX-R isoforms (Nav1.7, Nav1.8, Nav1.9), had high levels of peripherin but little NF200 or Necl-1. This expression pattern is consistent with small unmyelinated C-fibers such as those typically associated with thermoreception and pain. The large-diameter neurons (>30 μm) predominately expressed TTX-S Na currents, TTX-S Na channel isoforms (Nav1.1, Nav1.6, Nav1.7) and high levels of NF200 and Necl-1. This pattern is characteristic of rapidly-conducting myelinated A fibers sensitive to low-threshold non-noxious sensory stimulation. The data support the conclusion that small- and large-diameter DRG neurons differentially express Na channel isoforms with distinct voltage-dependence and gating properties that contribute to the unique electrical excitabilities of these neuronal populations.

Acknowledgments

The authors would like to thank Steve Malinowski for technical assistance. This work was supported by a grant from the National Institute of General Medical Sciences (GM078244).

Reference List

Akopian AN, Sivilotti L, Wood JN. A tetrodotoxin-resistant voltage-gated sodium channel expressed by sensory neurons. Nature 1996;379:257–262. [PubMed: 8538791]

Amaya F, Decosterd I, Samad TA, Plumpton C, Tate S, Mannion RJ, et al. Diversity of expression of the sensory neuron-specific TTX-resistant voltage-gated sodium ion channels SNS and SNS2. Mol Cell Neurosci 2000;15:331–342. [PubMed: 10845770]

Baker MD, Bostock H. Low-threshold, persistent sodium current in rat large dorsal root ganglion neurons in culture. J Neurophysiol 1997;77:1503–1513. [PubMed: 9084615]

Black JA, Dib-Hajj S, McNabola K, Jeste S, Rizzo MA, Kocsis JD, Waxman SG. Spinal sensory neurons express multiple sodium channel alpha-subunit mRNAs. Brain Res Mol Brain Res 1996;43:117–131. [PubMed: 9037525]

Black JA, Liu S, Tanaka M, Cummins TR, Waxman SG. Changes in the expression of tetrodotoxin-sensitive sodium channels within dorsal root ganglia neurons in inflammatory pain. Pain 2004;108:237–247. [PubMed: 15030943]

Blair NT, Bean BP. Roles of tetrodotoxin (TTX)-sensitive Na+ current, TTX-resistant Na+ current, and Ca2+ current in the action potentials of nociceptive sensory neurons. J Neurosci 2002;22:10277–10290. [PubMed: 12451128]

Caffrey JM, Eng DL, Black JA, Waxman SG, Kocsis JD. Three types of sodium channels in adult rat dorsal root ganglion neurons. Brain Res 1992;592:283–297. [PubMed: 1280518]

Choi JS, Tyrrell L, Waxman SG, Dib-Hajj SD. Functional role of the C-terminus of voltage-gated sodium channel Na(v)1.8. FEBS Lett 2004;572:256–260. [PubMed: 15304358]

Coste B, Osorio N, Padilla F, Crest M, Delmas P. Gating and modulation of presumptive NaV1.9 channels in enteric and spinal sensory neurons. Mol Cell Neurosci 2004;26:123–134. [PubMed: 15121184]

Cummins TR, Dib-Hajj SD, Black JA, Akopian AN, Wood JN, Waxman SG. A novel persistent tetrodotoxin-resistant sodium current in SNS-null and wild-type small primary sensory neurons. J Neurosci 1999;19:43.

Cummins TR, Sheets PL, Waxman SG. The roles of sodium channels in nociception: Implications for mechanisms of pain. Pain 2007;131:243–257. [PubMed: 17766042]

Dib-Hajj S, Black JA, Cummins TR, Waxman SG. NaN/Nav1.9: a sodium channel with unique properties. Trends Neurosci 2002;25:253–259. [PubMed: 11972962]

Dib-Hajj SD, Binshtok AM, Cummins TR, Jarvis MF, Samad T, Zimmermann K. Voltage-gated sodium channels in pain states: role in pathophysiology and targets for treatment. Brain Res Rev 2009;60:65–83. [PubMed: 19150627]

Dib-Hajj SD, Tyrrell L, Black JA, Waxman SG. NaN, a novel voltage-gated Na channel, is expressed preferentially in peripheral sensory neurons and down-regulated after axotomy. Proc Natl Acad Sci 1998;95:8963–8968. [PubMed: 9671787]

Djouhri L, Fang X, Okuse K, Wood JN, Berry CM, Lawson SN. The TTX-resistant sodium channel Nav1.8 (SNS/PN3): expression and correlation with membrane properties in rat nociceptive primary afferent neurons. J Physiol 2003;550:739–752. [PubMed: 12794175]

Elliott AA, Elliott JR. Characterization of TTX-sensitive and TTX-resistant sodium currents in small cells from adult rat dorsal root ganglia. J Physiol 1993;463:39–56. [PubMed: 8246189]

Fang X, Djouhri L, Black JA, Dib-Hajj SD, Waxman SG, Lawson SN. The presence and role of the tetrodotoxin-resistant sodium channel Na(v)1.9 (NaN) in nociceptive primary afferent neurons. J Neurosci 2002;22:7425–7433. [PubMed: 12196564]

Fjell J, Hjelmstrom P, Hormuzdiar W, Milenkovic M, Aglieco F, Tyrrell L, et al. Localization of the tetrodotoxin-resistant sodium channel NaN in nociceptors. Neuroreport 2000;11:199–202. [PubMed: 10683857]

Fornaro M, Lee JM, Raimondo S, Nicolino S, Geuna S, Giacobini-Robecchi M. Neuronal intermediate filament expression in rat dorsal root ganglia sensory neurons: an in vivo and in vitro study. Neuroscience 2008;153:1153–1163. [PubMed: 18434031]

Fuchs E, Cleveland DW. A structural scaffolding of intermediate filaments in health and disease. Science 1998;279:514–519. [PubMed: 9438837]

Fukuoka T, Kobayashi K, Yamanaka H, Obata K, Dai Y, Noguchi K. Comparative study of the distribution of the alpha-subunits of voltage-gated sodium channels in normal and axotomized rat dorsal root ganglion neurons. J Comp Neurol 2008;510:188–206. [PubMed: 18615542]

Goldstein ME, House SB, Gainer H. NF-L and peripherin immunoreactivities define distinct classes of rat sensory ganglion cells. J Neurosci Res 1991;30:92–104. [PubMed: 1795410]

Hamada K, Matsuura H, Sanada M, Toyoda F, Omatsu-Kanbe M, Kashiwagi A, Yasuda H. Properties of the Na+/K+ pump current in small neurons from adult rat dorsal root ganglia. Br J Pharmacol 2003;138:1517–1527. [PubMed: 12721107]

Harper AA, Lawson SN. Conduction velocity is related to morphological cell type in rat dorsal root ganglion neurones. J Physiol 1985;359:31–46. [PubMed: 3999040]

Herzog RI, Cummins TR, Ghassemi F, Dib-Hajj SD, Waxman SG. Distinct repriming and closed-state inactivation kinetics of Nav1.6 and Nav1.7 sodium channels in mouse spinal sensory neurons. J Physiol 2003;551:741–750. [PubMed: 12843211]

Hoffman PN, Cleveland DW, Griffin JW, Landes PW, Cowan NJ, Price DL. Neurofilament gene expression: a major determinant of axonal caliber. Proc Natl Acad Sci U S A 1987;84:3472–3476. [PubMed: 3472217]

Hoffman PN, Thompson GW, Griffin JW, Price DL. Changes in neurofilament transport coincide temporally with alterations in the caliber of axons in regenerating motor fibers. J Cell Biol 1985;101:1332–1340. [PubMed: 2413041]

Jarvis MF, Honore P, Shieh CC, Chapman M, Joshi S, Zhang XF, et al. A-803467, a potent and selective Nav1.8 sodium channel blocker, attenuates neuropathic and inflammatory pain in the rat. Proc Natl Acad Sci U S A 2007;104:8520–8525. [PubMed: 17483457]

John VH, Main MJ, Powell AJ, Gladwell ZM, Hick C, Sidhu HS, et al. Heterologous expression and functional analysis of rat Nav1.8 (SNS) voltage-gated sodium channels in the dorsal root ganglion neuroblastoma cell line ND7-23. Neuropharmacology 2004;46:425–438. [PubMed: 14975698]

Kakunaga S, Ikeda W, Itoh S, guchi-Tawarada M, Ohtsuka T, Mizoguchi A, Takai Y. Nectin-like molecule-1/TSLL1/SynCAM3: a neural tissue-specific immunoglobulin-like cell-cell adhesion molecule localizing at non-junctional contact sites of presynaptic nerve terminals, axons and glia cell processes. J Cell Sci 2005;118:1267–1277. [PubMed: 15741237]

Kostyuk PG, Veselovsky NS, Tsyndrenko AY. Ionic currents in the somatic membrane of rat dorsal root ganglion neurons-I. Sodium currents. Neuroscience 1981;6:2423–2430. [PubMed: 6275294]

Lai J, Porreca F, Hunter JC, Gold MS. Voltage-gated sodium channels and hyperalgesia. Annu Rev Pharmacol Toxicol 2004;44:371–397. [PubMed: 14744251]

Lasek RJ, Oblinger MM, Drake PF. Molecular biology of neuronal geometry: expression of neurofilament genes influences axonal diameter. Cold Spring Harb Symp Quant Biol 1983;48(Pt 2):731–744. [PubMed: 6202455]

Lawson SN. Phenotype and function of somatic primary afferent nociceptive neurones with C-, Adeltaor Aalpha/beta-fibres. Exp Physiol 2002;87:239–244. [PubMed: 11856969]

Lawson SN, Perry MJ, Prabhakar E, McCarthy PW. Primary sensory neurones: neurofilament, neuropeptides, and conduction velocity. Brain Res Bull 1993;30:239–243. [PubMed: 7681350]

Lawson SN, Waddell PJ. Soma neurofilament immunoreactivity is related to cell size and fibre conduction velocity in rat primary sensory neurons. J Physiol 1991;435:41–63. [PubMed: 1770443]

Lee KH, Chung K, Chung JM, Coggeshall RE. Correlation of cell body size, axon size, and signal conduction velocity for individually labelled dorsal root ganglion cells in the cat. J Comp Neurol 1986;243:335–346. [PubMed: 3950079]

Leffler A, Reiprich A, Mohapatra DP, Nau C. Use-dependent block by lidocaine but not amitriptyline is more pronounced in tetrodotoxin (TTX)-Resistant Nav1.8 than in TTX-sensitive Na+ channels. J Pharmacol Exp Ther 2007;320:354–364. [PubMed: 17005919]

Maurel P, Einheber S, Galinska J, Thaker P, Lam I, Rubin MB, et al. Nectin-like proteins mediate axon Schwann cell interactions along the internode and are essential for myelination. J Cell Biol 2007;178:861–874. [PubMed: 17724124]

Novakovic SD, Tzoumaka E, McGivern JG, Haraguchi M, Sangameswaran L, Gogas KR, et al. Distribution of the tetrodotoxin-resistant sodium channel PN3 in rat sensory neurons in normal and neuropathic conditions. J Neurosci 1998;18:2174–2187. [PubMed: 9482802]

Perry MJ, Lawson SN, Robertson J. Neurofilament immunoreactivity in populations of rat primary afferent neurons: a quantitative study of phosphorylated and non-phosphorylated subunits. J Neurocytol 1991;20:746–758. [PubMed: 1960537]

Priest BT, Murphy BA, Lindia JA, Diaz C, Abbadie C, Ritter AM, et al. Contribution of the tetrodotoxin-resistant voltage-gated sodium channel NaV1.9 to sensory transmission and nociceptive behavior. Proc Natl Acad Sci U S A 2005;102:9382–9387. [PubMed: 15964986]

Renganathan M, Cummins TR, Hormuzdiar WN, Waxman SG. alpha-SNS produces the slow TTX-resistant sodium current in large cutaneous afferent DRG neurons. J Neurophysiol 2000;84:710–718. [PubMed: 10938298]

Roy ML, Narahashi T. Differential properties of tetrodotoxin-sensitive and tetrodotoxin-resistant sodium channels in rat dorsal root ganglion neurons. J Neurosci 1992;12:2104–2111. [PubMed: 1318956]

Rush AM, Cummins TR, Waxman SG. Multiple sodium channels and their roles in electrogenesis within dorsal root ganglion neurons. J Physiol 2007;579:1–14. [PubMed: 17158175]

Sangameswaran L, Delgado SG, Fish LM, Koch BD, Jakeman LB, Stewart GR, et al. Structure and function of a novel voltage-gated, tetrodotoxin-resistant sodium channel specific to sensory neurons. J Biol Chem 1996;271:5953–5956. [PubMed: 8626372]

Sangameswaran L, Fish LM, Koch BD, Rabert DK, Delgado SG, Ilnicka M, et al. A novel tetrodotoxin-sensitive, voltage-gated sodium channel expressed in rat and human dorsal root ganglia. J Biol Chem 1997;272:14805–14809. [PubMed: 9169448]

Spiegel I, Adamsky K, Eshed Y, Milo R, Sabanay H, Sarig-Nadir O, et al. A central role for Necl4 (SynCAM4) in Schwann cell-axon interaction and myelination. Nat Neurosci 2007;10:861–869. [PubMed: 17558405]

Tate S, Benn S, Hick C, Trezise D, John V, Mannion RJ, et al. Two sodium channels contribute to the TTX-R sodium current in primary sensory neurons. Nat Neurosci 1998;1:653–655. [PubMed: 10196578]

Toledo-Aral JJ, Moss BL, He ZJ, Koszowski AG, Whisenand T, Levinson SR, et al. Identification of PN1, a predominant voltage-dependent sodium channel expressed principally in peripheral neurons. Proc Natl Acad Sci U S A 1997;94:1527–1532. [PubMed: 9037087]

Vijayaragavan K, O'Leary ME, Chahine M. Gating properties of Na(v)1.7 and Na(v)1.8 peripheral nerve sodium channels. J Neurosci 2001;21:7909–7918. [PubMed: 11588164]

Yoshida S, Matsuda Y. Studies on sensory neurons of the mouse with intracellular-recording and horseradish peroxidase-injection techniques. J Neurophysiol 1979;42:1134–1145. [PubMed: 479922]

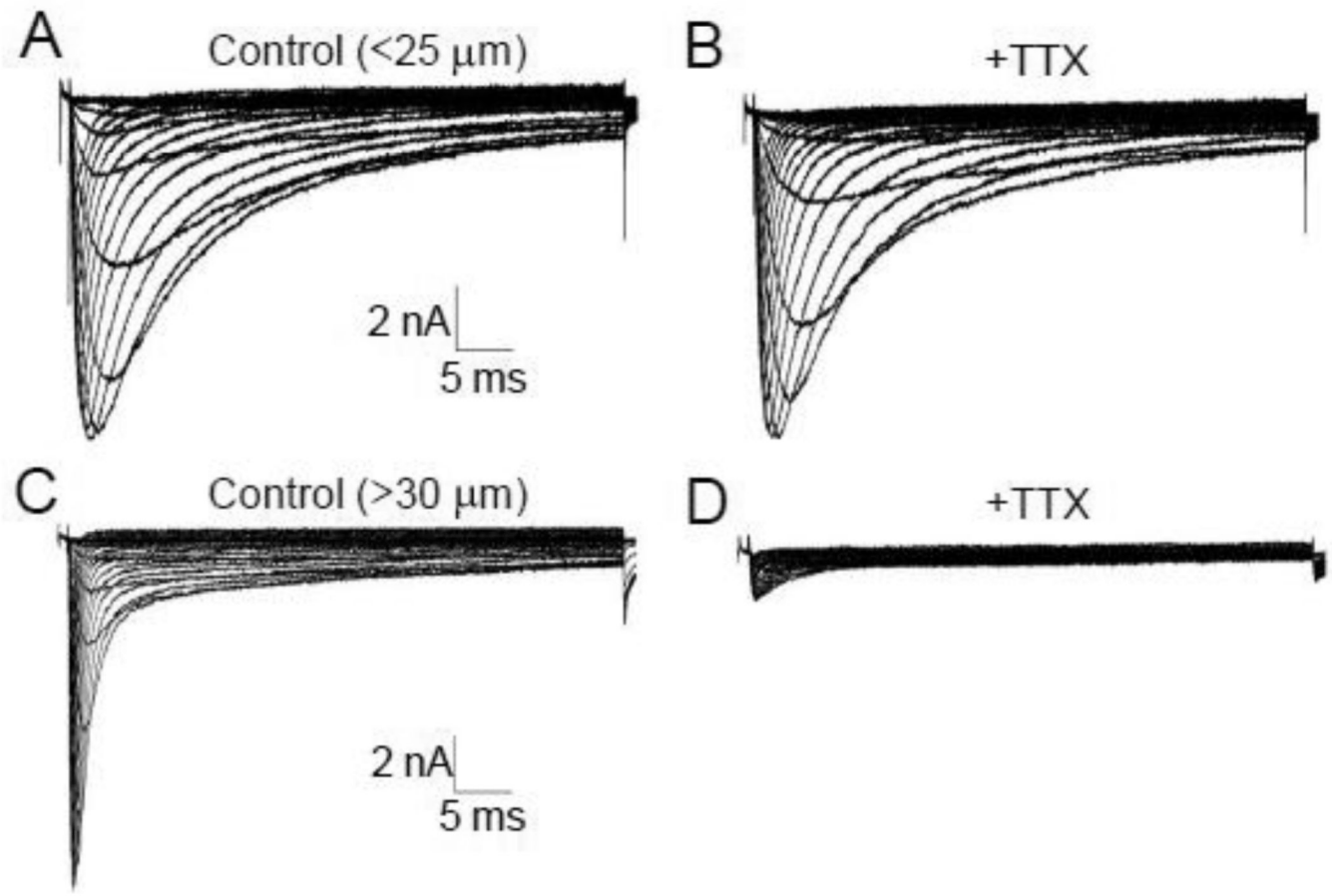

Figure 1. Na currents of small and large DRG neurons

A, C, Control Na currents of a small- (25 µm) and a large-diameter (35 µm) DRG neurons elicited by voltage pulses between −70 and +15 mV from a holding potential of −80 mV. Hyperpolarizing prepulses (−120 mV/500 ms) were applied immediately prior to the test pulses to fully activate the Na channels. **B, D,** Na currents recorded from the same small (Panel C) and large (Panel D) neurons after bath application of 300 nM tetrodotoxin (+TTX).

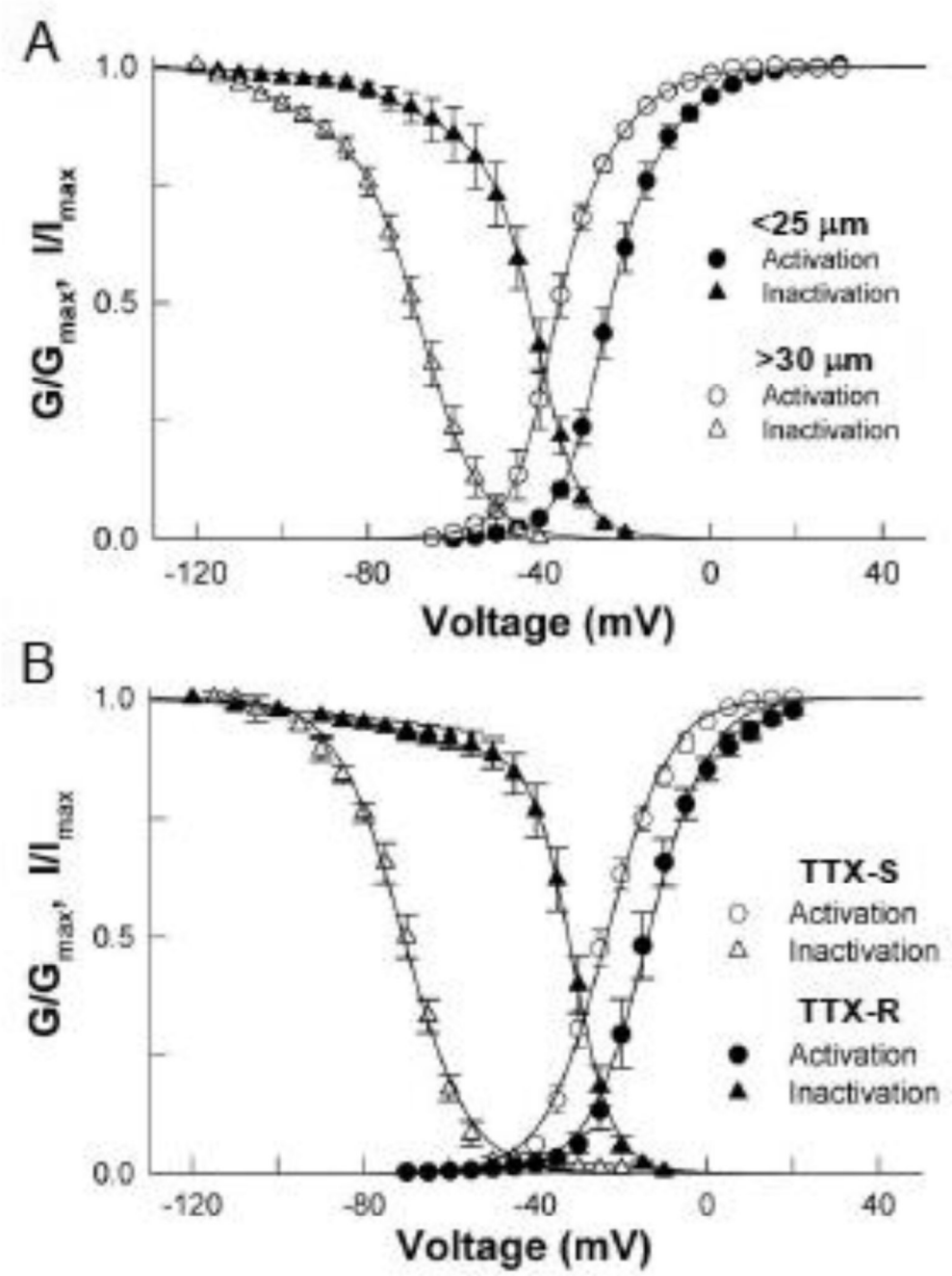

Figure 2. Voltage-dependent gating of DRG Na currents

A. The normalized conductance (G/G_{max}) was calculated from the peak currents and plotted versus the test potential. The smooth curves are fits of the data to a double Boltzmann function with midpoints (V_{act}) of −25.9 ± 0.5 mV (A=0.64) and −14.5 ± 3.6 mV for small the (n=12) and −38.2 ± 0.4 mV (A=0.50) and −28.8 ± 1.5 mV (n=8) for the large neurons. The steady-state inactivation was determined using 500 ms prepulses to the indicated voltages and the normalized (I/I_{max}) test current amplitudes (20 mV/50 ms) plotted versus the prepulse voltage. The smooth curves are fits to a double Boltzmann with midpoints (V_{in}) of −65.7 ± 7.0 mV (A=0.21) and −40.5 ± 0.2 mV for the small (n=12) and −103.2 ± 0.4 mV (A=0.11) and −67.7 ± 0.4 mV for the large neurons (n=8) where A is the relative amplitude

of the more hyperpolarized component. **B.** Gating properties of the isolated TTX-S and TTX-R Na currents. TTXS currents of large neurons were obtained by subtracting the residual TTX-R current measured after bath application of 300 nM TTX from the total current. The TTX-R currents of small neurons were directly measured after inhibiting TTX-S Na currents with 300 nM TTX. The normalized conductance and steady-state inactivation were plotted versus the test potential. The smooth curves are Boltzmann fits with midpoints (V_{act}) and slope factors (k) of −23.4 ±1.2 mV and 7.1 ± 0.3 mV (n=8) for the TTX-S current and −11.8 ± 1.3 mV and 6.2 ± 0.5 mV (n=9) for the TTX-R current. The steady-state inactivation of the TTX-S current was fitted with a midpoint and slope factor of −67.4 ± 1.3 mV and 7.5 ± 0.3 mV (n=7). The inactivation of the TTX-R current was fitted with a double Boltzmann with midpoints and slope factors of −76.3 ± 4.5 mV (A=0.10) and 16.4 ± 1.3 mV for the more hyperpolarized component and −30.3 ± 1.0 mV and 4.0 ± 0.02 mV (A=0.90) for the depolarized component (n=9).

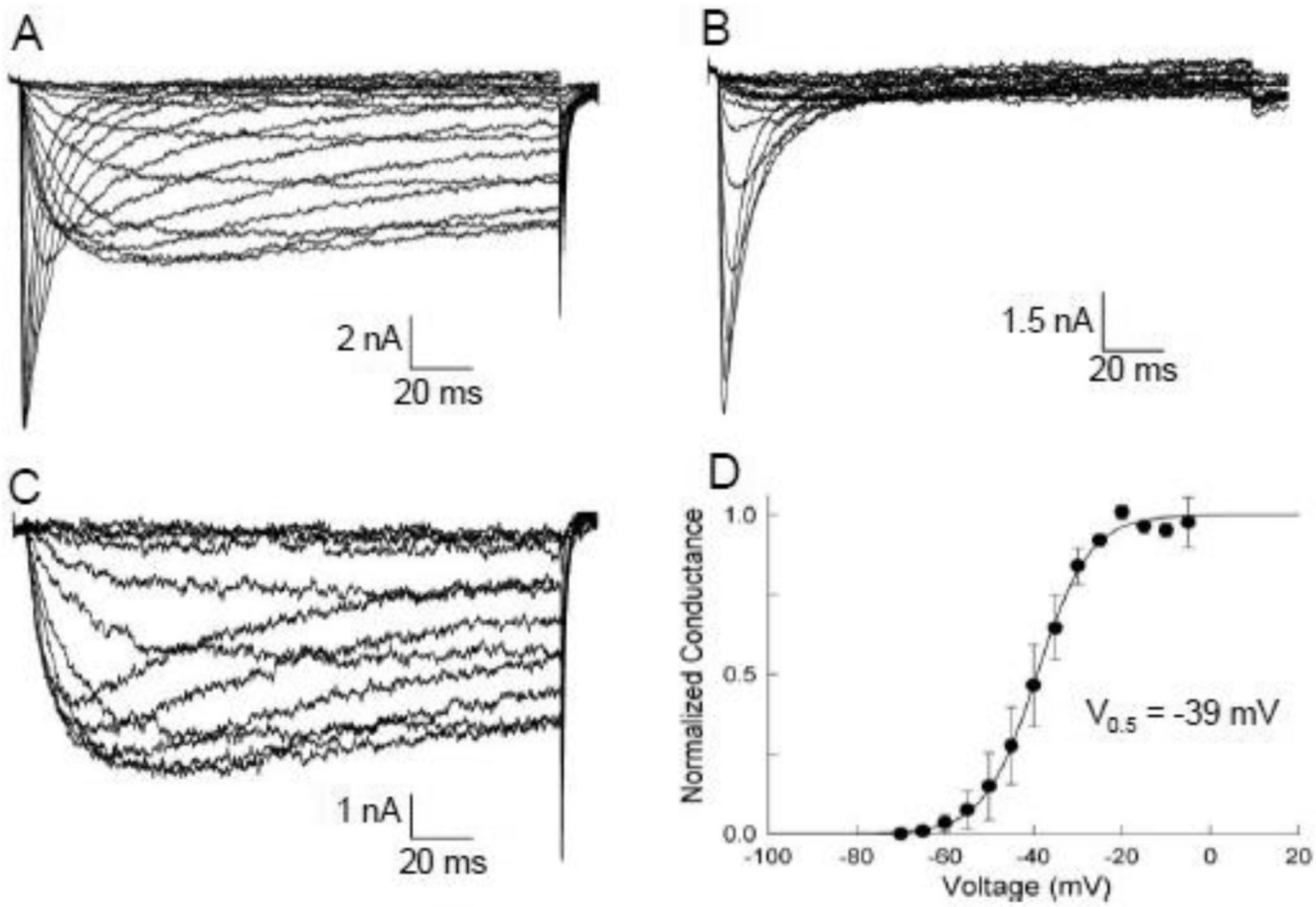

Figure 3. Voltage-dependent gating of the persistent TTX-R Na current

A. Total Na current of a small-diameter (21 μm) DRG neuron. Current was elicited by depolarizing pulses between −80 and 0 mV from a holding potential of −100 mV. A-803467 (1 μM) was included in the extracellular solution to selectively reduce the amplitude of Nav1.8 currents. **B**. Currents recorded from the same neuron as panel A using a holding potential of −60 mV. A short hyperpolarizing prepulse (−140 mV/25 ms) applied immediately prior to the test pulses permitted the full recovery of the rapidly inactivating component. **C**. Persistent TTX-R current obtained by subtracting the rapidly-inactivating component (Panel B) from the total current (Panel A). **D**. Normalized conductance (G/G_{max}) of the persistent TTX-R Na current plotted versus the test voltage. The smooth current is the fit to a Boltzmann function with midpoint ($V_{0.5}$) and slope factor (k) of −39.3 ± 0.3 mV and 5.9 ± 0.2 mV (n=8).

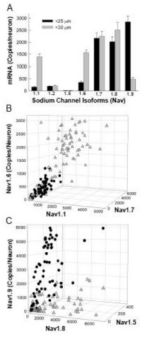

Figure 4. Expression of Na channel transcripts in DRG neurons

A. Small- (<25 μm) and large-diameter (>30 μm) neurons were individually harvested. The mRNA present in the cell lysates was reverse transcribed and quantitated (mRNA copies/ neuron) determined using Taqman real-time PCR. The data are the means and standard errors of 71 small and 90 large neurons. These data are summarized in Table 1. **B**. The mRNA encoding for TTX-S Na channels (Nav1.1, Nav1.6, Nav1.7) were measured from the same group of neurons. The mRNA copy numbers of the small (circles) and large (triangles) neurons are shown as three dimensional scatter plots. **C**. Scatter plot of the TTX-R Na channel mRNA (Nav1.5, Nav1.8, Nav1.9) of small (circles) and large (triangles) neurons.

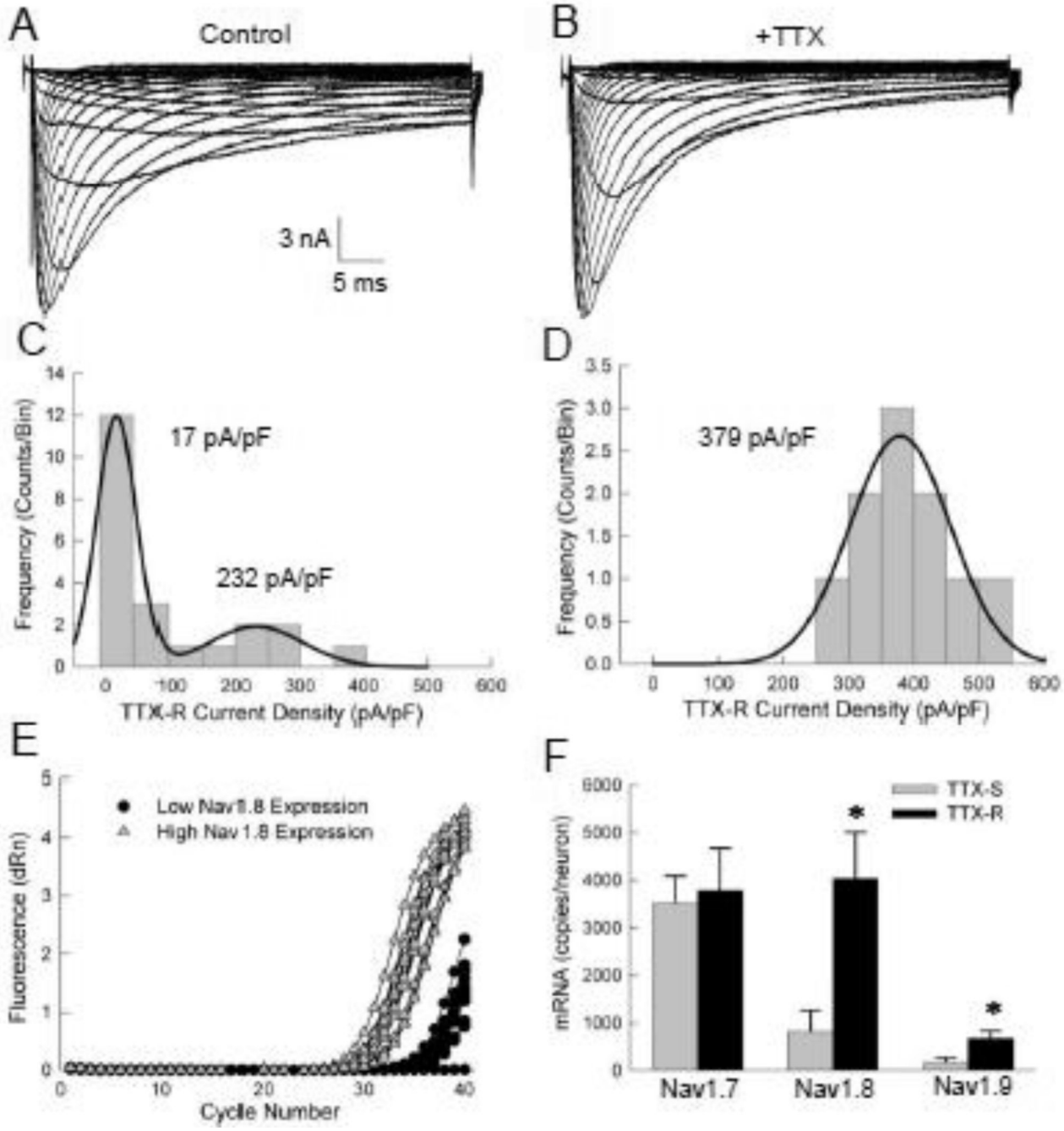

Figure 5. Expression of TTX-R Na current in large neurons

A, B, Whole-cell Na currents of a large-diameter (40 μm) neuron elicited by test pulses between −70 and +15 mV from a holding potential of −80 mV. A hyperpolarizing prepulse (−120 mV/500 ms) was applied immediately before the test pulses. Currents were recorded in the absence (Control) and after bath application of 300 nM TTX (+TTX). **C, D,** The peak current amplitudes at +20 mV were normalized to the whole-cell capacitance and plotted as a frequency histogram. The smooth curves are fits to Gaussian functions with peaks at 17 and 232 pA/pF for large neurons and 379 pA/pF for the small neurons. **E.** Real-time PCR amplification curves of Nav1.8 mRNA from 29 large neurons showing two distinct expression levels. Data are summarized in Table 1. **F**. The TTX sensitivities of large

neurons were determined using electrophysiology before harvesting and mRNA analysis. Histograms compare the Na channel mRNA copy numbers of neurons preferentially expressing either TTX-S or TTX-R Na current (n=10). The large neurons displaying TTX-R current also highly expressed NF200 (3789 ± 834 copies/neuron) and Necl-1 (10,112 ± 3184 copies/neuron, n=10).

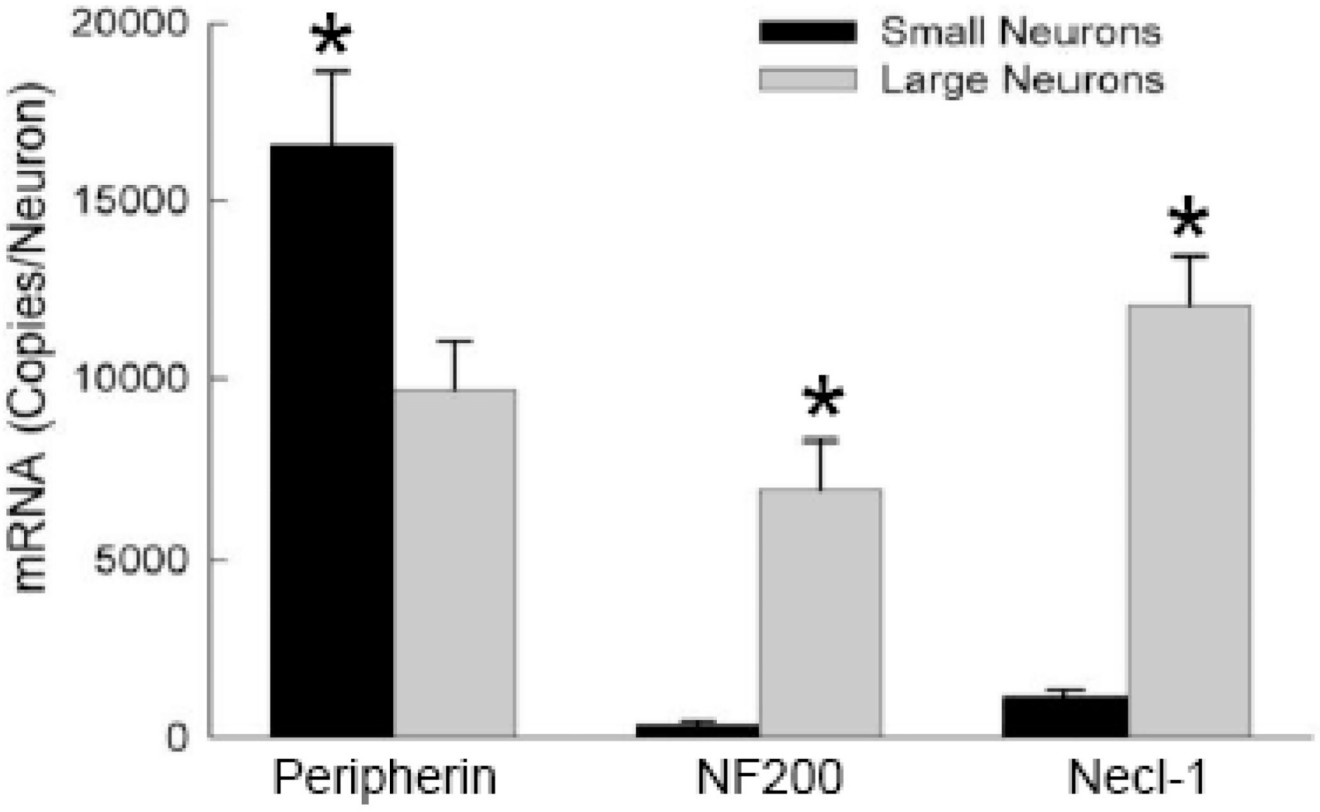

Figure 6. Expression of peripherin, NF200 and Necl-1

Small and large neurons were harvested and assayed for neurofilaments (peripherin, NF200) and Necl-1 mRNA. Data are the means and standard errors of 30 large and 23 small neurons. Asterisks indicate significant differences using student t-test ($p<0.05$).

Table 1

mRNA Expression(Copies per Neuron)

	Small	Large
Nav 1.1	159 ± 23	1398 ± 122
Nav 1.2	195 ± 22	209 ± 23
Nav 1.5	11 ± 5	10 ± 6
Nav 1.6	355 ± 49	1564 ± 114
Nav 1.7	2168 ± 223	2253 ± 197
Nav 1.8	2021 ± 213	819 ± 445*
		4042 ± 965
Nav 1.9	2254 ± 238	489 ± 80

Data are the means and SEM of 71 and 90 small and large neurons respectively.

* The majority of large neurons (78%) expressed Nav1.8 at a low level. The higher copy number was observed in a small subpopulation of the large neurons (Figure 5F).